

Weak phase stiffness and nature of the quantum critical point in underdoped cuprates

Yucel Yildirim^{1,*} and Wei Ku (顧威)^{1,2,†}

¹*CMPMSD, Brookhaven National Laboratory, Upton, NY 11973-5000, U.S.A.*

²*Physics Department, State University of New York, Stony Brook, New York 11790, USA*

(Dated: March 1, 2013)

We demonstrate that the zero-temperature superconducting phase diagram of underdoped cuprates can be quantitatively understood in the strong binding limit, using only the experimental spectral function of the “normal” pseudo-gap phase without any free parameter. In the prototypical $(\text{La}_{1-x}\text{Sr}_x)_2\text{CuO}_4$, a kinetics-driven d -wave superconductivity is obtained above the critical doping $\delta_c \sim 5.2\%$, below which complete loss of superfluidity results from local quantum fluctuation involving local p -wave pairs. Near the critical doping, a enormous mass enhancement of the local pairs is found responsible for the observed rapid decrease of phase stiffness. Finally, a striking mass divergence is predicted at δ_c that dictates the occurrence of the observed quantum critical point and the sudden suppression of the Nernst effects in the nearby region.

PACS numbers: 74.72.-h, 74.20.Mn, 74.40.Kb, 74.20.Rp

Considering the enormous amount of research activities devoted to the problem of high- T_c superconductivity, it is hardly an exaggeration to regard it as one of today’s most important unsolved problems in physics. Specifically in the underdoped region, it is now commonly accepted that the low carrier density in the system necessarily leads to strong phase fluctuation of the superconducting order parameter[1] due to its conjugate nature to the number fluctuation. Consequently, the transition temperature T_c is suppressed significantly below the pairing energy scale that controls all essential aspects of the standard theory of superconductivity[2]. The crucial role of phase fluctuation[1, 3, 4] has recently gained significant support from various experiments[5–7] in both the low-temperature superconducting state and the ‘normal state’ above the transition temperature T_c , and is likely tied closely to many of the exotic properties[1, 8–12] in this region.

Nonetheless, besides this general understanding, several key issues remain puzzling in the underdoped region. In spite of an uneventful evolution of the one-particle spectral function[11], the superfluid density reduces *dramatically* near the observed quantum critical point (QCP)[13] (at the critical doping $\delta_c \sim 5.2\%$ for doped La_2CuO_4), below which superconductivity ceases to exist even at zero temperature. The current consideration of phase fluctuation [1] would only indicate softer phase at lower carrier density, but offer no explanation for the complete suppression of superconductivity at zero temperature at $\delta < \delta_{QCP}$. Particularly in La_2CuO_4 , δ_{QCP} is quite far away from the antiferromagnetic (AF) phase boundary, rendering the common consideration of competing order unsatisfactory. This vanishing of superconductivity below δ_c , the nature of the QCP, the dramatic reduction of superfluid density nearby, and the controlling factor of the value of δ_c , all remain challenging to our basic understanding.

Perhaps the most puzzling observation is the sudden

suppression of the observed Nernst effect at $T > T_c$ around the same critical doping δ_c [14]. This indicates that not only the long-range phase coherence, but also the short-range phase coherence is lost near the QCP, a phenomenon unexplainable via simple fluctuation scenario, for example due to low dimensionality.

In this letter, we demonstrate that these puzzles can be quantitatively understood in the strong pairing limit of local pairs of doped holes. We obtain the zero-temperature phase diagram with no need for any free parameter other than the experimental one-particle spectral function of the “normal” pseudo-gap state. A kinetics-driven d -wave condensate is found at $\delta > \delta_c$, with a largely enhanced bosonic mass, $m_b > 40m_e$. In great contrast, ground states consisting of fluctuating p -wave pairs are found at $\delta < \delta_c$, incapable of sustaining a condensate. At $\delta = \delta_c$, a mass divergence results from the degeneracy of local d - and p -wave symmetry, dictating the presence of QCP. Correspondingly, near QCP $\delta \leq \delta_c$, the diverging mass explains the puzzling dramatic reduction of phase stiffness in both long-range and short-range. Our study provides a novel yet simple paradigm to the behavior of local pairs in underdoped cuprates, and is expected to inspire new set of experimental confirmation, as well as re-interpretation of existing experimental observations.

Conceptually, a phase-fluctuation dominant superconductivity hosts relatively negligible amplitude fluctuation of the order parameter at low energy/temperature. This implies that the effective low-energy Hamiltonian for the charge and pairing channels must have integrated out all pair-breaking processes to conserve the amplitude of the order parameter, for example, as in the x - y model[15]. The higher-energy pairing energy scale should then manifest itself only through a strong “pair-preserving” constraint of the low-energy Hamiltonian. This is in perfect analogy to the replacement of repulsion U of the Hubbard model by a “no double occupancy” constraint in

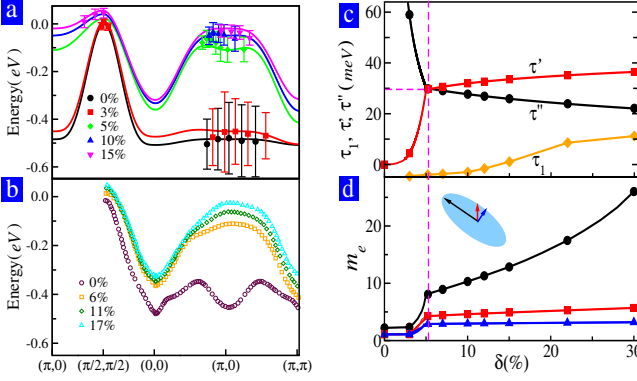


FIG. 1: (Color online) Band dispersion from experiment, our fitting (a), and the t - J model[20] (b), and the corresponding parameters τ , τ' and τ'' (c). (d) Weak doping dependence of the effective mass of doped holes m_h^* in different directions indicated by the arrows in the inset.

its lower energy counterparts, say the t - J model. Consequently, a new paradigm for the low-energy physics emerges at $T \leq T_c$, which differs completely from the amplitude fluctuation of the standard theories. In this new physical regime, the detail of the pairing mechanisms (AF correlation[16, 17], spin-fluctuation[18], or formation of bi-polaron[19]) are no longer essential. Instead, the physics is now dominated by the effective kinetic energy that controls the phase coherence. Since only one energy scale is essential in this regime, the low-energy physics should be universal and simple.

We then proceed to derive the effective motion of the local pairs in three steps: 1) obtaining the effective kinetics of the doped holes from the experimental one-particle spectral function in the “normal state” pseudogap phase, 2) splitting the many-body Hilbert space between unpaired and paired holes, and 3) re-represent the effective kinetics to reveal the motion and scattering of unpaired and paired holes. The resulting pivoting motion of the pairs would then lead straightforwardly to all our quantitative conclusions without any free parameter.

Let’s define the irreducible effective kinetic kernel τ of the low-energy carriers, $\tau = G_L^{-1} - G^{-1}$ (in matrix notation), through the measured one-particle propagator G and a non-propagating Green’s function G_L consisting of a single pole at the central energy of the band. The real part of τ thus controls the propagation of the carriers, with offdiagonal elements giving the dispersion, like the effective hopping matrix elements. The imaginary part of τ gives the decay of carriers and will be ignored in this study, since only the average motion is of interest. The dispersion in the measured G can then be captured by

$$H = \sum_{ii'} \tau_{ii'} c_i^\dagger c_{i'} + h.c. \quad (1)$$

Note that this Hamiltonian is only meant to represent the average effective kinetics of the fully renormalized

one-particle propagator, within the low-energy “pair-preserving” constraint. It certainly does not contain information of the pairing interaction that connects to the high-energy sector, or the scattering process that broadens the spectral function. Therefore, τ is to be distinguished from the “bare” hopping parameter t commonly used in the Hubbard or t - J model, as τ have fully absorbed the effects of interactions and constraints.

Fig. 1(a) shows the dispersion of the main features in the measured spectral functions of $(\text{La}_{1-x}\text{Sr}_x)_2\text{CuO}_4$ by angular-resolved photoemission spectroscopy (ARPES)[21, 22]. Also shown are the dispersion obtained by diagonalizing Eq. 1 using τ as fitting parameters. One notices immediately the well-known observation that the dispersion is not rigid against the doping level. The close resemblance to the previously published t - J model solutions[20] in Fig. 1(b) suggests that this strong doping-dependent renormalization originates primarily from the competition between the bare kinetic energy and the AF interaction. Consequently, the resulting fully-renormalized first, second and third neighbor kernels, τ_1 , τ' and τ'' demonstrate strong doping dependence as well (Fig. 1(c)). Interestingly, as δ decreases, τ'' is found to increase steadily approaching the value of τ' , and then exceeds τ' right at δ_{QCP} ! This is apparently not a coincidence, and reveals an important clue to the nature of QCP to be discussed below. Since the fully dressed τ_1 is negligibly small at the underdoped regime, understandable from the strong antiferromagnetic correlation, it will be dropped from our further analysis. As a reference, Fig. 1(d) also shows the effective mass of the doped holes, m_h^* , in three directions. In agreement with the experimental observation[23], m_h^* is about constant for $\delta > 5.2\%$.

Next, we split rigorously the many-body Hilbert space into two components [24]: one spanned by the tightly bound pairs of nearest neighboring holes, $b_{ij}^\dagger = c_{i\uparrow}^\dagger c_{j\downarrow}^\dagger$, and the other by the unpaired holes, $f_{i\sigma}^\dagger$:

$$\begin{aligned} c_{i\uparrow}^\dagger &= f_{i\uparrow}^\dagger + \sum_{j \in NN(i)} b_{ij}^\dagger f_{j\downarrow} + [b^\dagger b^\dagger b f + \dots] \\ c_{j\downarrow}^\dagger &= f_{j\downarrow}^\dagger - \sum_{i \in NN(j)} b_{ij}^\dagger f_{i\uparrow} + [b^\dagger b^\dagger b f + \dots] \end{aligned} \quad (2)$$

where \sum' denotes “sum only the first non-zero term” to avoid double counting [24]. Such a real-space hole pair can result from the strong AF correlation[4, 25, 26] or the formation of bi-polaron[19], but is to be distinguished from the real-space singlet pair of electron commonly used in the RVB-like construction[27]. Since our study will focus only on the charge and pairing channels, for a cleaner presentation, the spin indices and the associated sign changes will be suppressed from now on.

Finally, ignoring the higher order terms owing to the

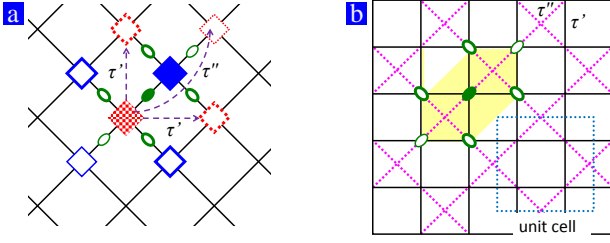


FIG. 2: (Color online) Illustration of kinetic processes of a pair of holes (filled diamond) to its six allowed destinations (open diamonds) under the “pair-preserving” constraint (a), through τ' (solid lines) and τ'' (dashed lines). The same is alternatively represented by ellipsoids denoting a pair and its allowed destinations in the lattice of bond-centered pairs (b). The yellow area denotes the region of the ‘extended hardcore constraint’ that excludes other pairs. The dotted square gives the convenient unit cell in our calculations.

low carrier density, and inserting Eq. 2 into Eq. 1, we re-represent the carrier kinetics as $H = H^b + H^f + H^{bf}$ [24] (dropping the redundant $f_j f_j^\dagger$ in $b_{ij}^\dagger f_j f_j^\dagger b_{i'j}$), where

$$H^b = \sum_{ii'j} \tau_{ii'} b_{ij}^\dagger b_{i'j} + h.c. \quad (3)$$

describes the pivoting motion of the pairs. The remaining terms H^f and H^{bf} give the motion of unpaired holes and their coupling to the pairs [24]. In essence, this representation merely reveals the internal processes embedded in the experimentally observed one-particle propagator.

The resulting pivoting motion of the paired holes is illustrated in Fig. 2. Consider a single pair of holes (blue and red filled diamonds) located in the fermion lattice in Fig. 2(a). Under the pair-preserving constraint, only three potential destinations (empty diamonds) for each hole are allowed. Converting to the lattice of bond-centered pairs in Fig. 2(b), one finds two inequivalent sites in a square lattice, each of which can hop to four first neighboring sites with τ' , but to only *two* second neighboring sites with τ'' along their designated direction (denoted by the direction of the ellipsoids). As we will present elsewhere, this pivoting motion of the pair can actually be derived more completely to include both the real and imaginary part of τ via the equation of motion. Alternatively, one can also arrive at the same via the ladder diagrams in the strong binding limit in perturbation theory.

Note that the hole pairs b 's are under a strong ‘extended hardcore constraint’: $b_{ij}^\dagger b_{i'j'}^\dagger = 0$ if $i = i'$ or $j = j'$. This is inherited from the Pauli exclusion principle of the original fermion operators $c_{i\sigma}^\dagger c_{i\sigma}^\dagger = 0$ and that double occupancy of electrons are not allowed in the low-energy sector. In Fig. 2(b), this constraint forbids occupation of the six potential hopping destinations of each pair by another pair. Therefore, these real-space pairs are correlated via a “polite” policy that no one is to get

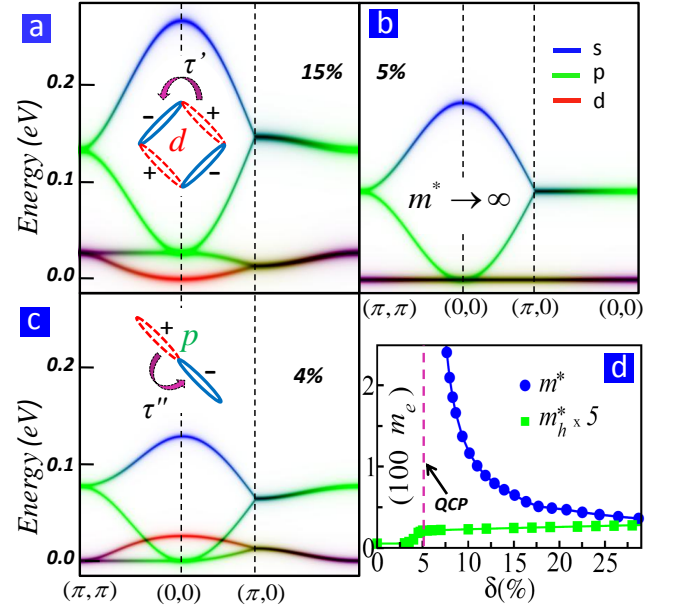


FIG. 3: (Color online) The band dispersion of the hole pairs without the extended hardcore constraint, at $\delta > \delta_{QCP}$ (a), $\delta = \delta_{QCP}$ (b), and $\delta < \delta_{QCP}$ (c). Insets in (a) and (c) illustrate the Wannier function corresponding to the lowest band, and the kinetic driving force for the local symmetry. (d) Strongly enhanced effective mass of the pairs, m^* , and the doped holes, m_h^* .

into others’ immediate hopping path. This constraint can be considered as an infinite short-range repulsion that dominates the inter-pair interactions in most cases, and is responsible for stabilizing our bosonic system against potential phase separation[28].

Now, we will show that this rigorously derived, simple Hamiltonian gives *quantitatively* all the above mentioned essential aspects of superfluid in underdoped cuprates, without any free parameter. For convenience, a unit cell is chosen to include four sites as shown in Fig. 2(b). This choice explicitly allows one s-, two p-, and one d-wave superposition within the unit cell, and equates the doping level per unit cell in this lattice and that in the standard fermion lattice. Fig. 3(a) illustrates the resulting band structure of H^b at doping level of the superconducting phase $\delta = 15\% > \delta_{QCP}$ before including the extended hardcore constraint. It shows that at low enough temperature a Bose-Einstein condensate (BEC) would take place at a single minimum at momentum $q = 0$, with a pure d-wave symmetry (red color). As in standard dilute bosonic systems, one thus expects a d-wave superfluid with finite stiffness, once given a scattering length derived from the extended hardcore constraint.

The d-wave structure of the pair is better illustrated in real space via the corresponding Wannier function, computed from the Fourier transform of the Bloch functions of the lowest band. Fig. 3(a) shows that the low-energy pairs has clear d-wave symmetry with nodes along the

(π, π) directions of the standard Fermion lattice, in perfect agreement with the experimental observations.[11, 29, 30] (Notice that our fermionic lattice is rotated by 45° from the usual convention.)

We stress that our resulting local d -wave symmetry is completely driven by the *fully screened kinetic energy*. [31, 32] It originates from the dominance of *positive* τ' of the local pair, which prefers energetically opposite sign of the wave function across first neighbors, thus favoring a d -wave symmetry (see Fig. 3(a)). In comparison, the positive τ'' favors opposite sign across the second neighbors, thus p -wave symmetry (see Fig. 3(c)). Therefore, τ' and τ'' compete by lowering the band energy of d - and p -bands, respectively.

This explains the long-standing puzzle of lack of superconductivity at lower doping ($\delta < \delta_{QCP}$). Since in this region $\tau'' > \tau'$ [see Fig. 1(c)], Fig. 3(c) shows local p -wave pair has lower energy than d -wave pairs. Furthermore, the structure of the lattice in Fig. 2(b) dictates a line of degenerate p -states in momentum space along the anti-nodal directions. The pairs can therefore populate any arbitrary state along this line without ever forming a BEC. That is, the pairs in the system have local p -wave symmetry without possible global phase coherence, an effect of quantum fluctuation beyond the original consideration of thermal phase fluctuation [1]. These incoherent p -wave pairs might also offer a new paradigm to the insulating glassy behavior of the electronic structure in this region, for example the strong scattering in the charge channel.

The competition between d -wave and p -wave also offers a natural explanation of the dramatic phase softness and the low superfluid density of the underdoped cuprates. Indeed, even near the optimal doping ($\delta \approx 15\%$), the comparable value of τ'' and τ' leads to a large effective mass of the pair $m^* = (\hbar^2/l^2)d^2\epsilon_k/dk^2 \approx 12m_h^* \approx 59m_e$ (l being the lattice constant). This gives a rather long penetration depth $\lambda = \sqrt{\frac{m^*c^2}{4\pi e^2 n_s}} \approx 7000\text{\AA}$ (taking $n_s \sim \delta$ per unit cell), in reasonable agreement with the experimental value [33]. Furthermore, as δ approaches δ_{QCP} , τ'' grows to the value of τ' , reducing the separation of the d -band and the p -band, and in turn flattening the d -band. The effective mass of the d band thus increases significantly (Fig. 3(d)). Since the superfluid stiffness correlates with the inverse of the effective mass, the large mass enhancement dictates the observed very soft phase.

This analysis reveals the simple yet exotic nature of the observed QCP at the end of the underdoped superconductivity region $\delta_{QCP} = 5.2\%$: It is dictated by the diverged effective mass of the local pairs [Fig. 3(d)]. At this point $\tau' = \tau''$ and the d -wave and p -wave pairs become locally degenerate and the d -band is thus completely disperseless, as shown in Fig. 3(b). Since the effective mass now diverges [Fig. 3(c)], the pairs can no longer propagate and align the phase to develop a condensate even at

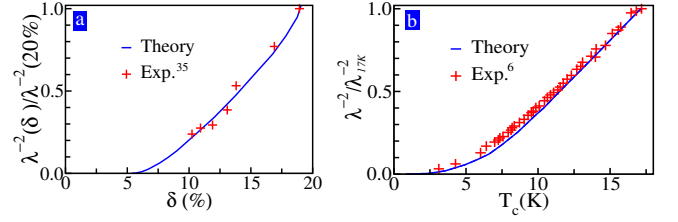


FIG. 4: (Color online) Experimental supports of predicted mass divergence via (a) non-linear doping dependence of inverse penetration depth and (b) non-linear correlation between inverse penetration depth and transition temperature T_c .

zero temperature. In essence, it is the perfect quantum mechanical interference between the first- and second-neighbor hopping that renders the local pairs immobile and in turn disables the phase coherence of superconductivity.

The diverged effective mass also account for the dramatic suppression of diamagnetic response near δ_{QCP} [34]. Indeed, the diverging effective mass would not only suppress the long-range phase coherence but also the shorter-range coherence responsible for a strong diamagnetic response. The observed dramatic reduction of the Nernst signal [14] near the QCP is thus understandable.

Our predicted mass divergence near QCP is actually strongly supported by experimental measurements of penetration depth λ of the underdoped $\text{YBa}_2\text{Cu}_3\text{O}_y$ samples. Figure 4(a) shows that over the entire underdoped region, the measured λ^{-2} [35] deviates significantly from the simple $\lambda^{-2} \propto \delta$ relationship to be expected if the effective mass is assumed constant. On the other hand, our theory with large doping-dependent effective mass reproduces very nicely the experimental observation. A even more direct evidence is provided by the recent measurement on the extremely underdoped $\text{YBa}_2\text{Cu}_3\text{O}_y$ samples near the QCP [6]. The observed relationship between low-temperature λ^{-2} and T_c in Fig. 4(b) shows a strong non-linear dependence. In fact, the same behavior has also been observed via mutual inductance[36]. The zero slope at $\lambda \rightarrow 0$ can be interpreted as an indirect evidence of the mass divergence, and our theory reproduces very nicely the experimental observation. (T_c is determined by thermally exhausting all the pairs $\int_\mu d\omega \text{DOS}(\omega)/(e^{\beta(T_c)\omega} - 1) = \delta$.) In addition, the mass divergence would also make sense the observed dramatic enhancement of the residual specific heat[37] and of the isotope effect[38] near the QCP. Nonetheless, a direct measurement of the superfluid inertia or the effective mass of the pair above T_c would be highly valuable.

In conclusion, we demonstrate that all the key feature of superconductivity in the underdoped cuprates can be described quantitatively in the strong binding limit, without use of any free parameter. The d -wave symmetry is found to originate from the renormalized kinetic energy, and the observed superconductivity can be understood

as a superfluid of a dilute real-space hole pairs. Our result explains the lack of superconductivity at $\delta < \delta_{QCP}$ via quantum fluctuation associated with incoherent local p -wave pairs. In the underdoped regime, a large effective mass enhancement of the hole pairs is found responsible for the observed weak phase stiffness. Finally, the observed $\delta = 5.2\%$ QCP is found dictated by the divergence of the effective mass of the hole pairs, which also make sense the dramatic reduction of diamagnetic response (the Nernst effect) near the QCP. These successes support strongly a simple description of phase fluctuating dominant superfluidity for the underdoped cuprates and enable further reconciliation of seemingly contradicting experimental conclusions in the field.

We acknowledge useful discussions with Maxim Khodas and Chris Homes, and comments from Alexei Tsvelik and Weiguo Yin. This work was supported by the U.S. Department of Energy, Office of Basic Energy Science, under Contract No. DE-AC02-98CH10886.

* current address: Physics Department, Faculty of Arts and Sciences, Doğuş University, Acıbadem-Kadıköy, 34722 Istanbul, Turkey

† corresponding email: weiku@bnl.gov

- [1] V. J. Emery and S. A. Kivelson, *Nature* **374**, 434 (1995).
- [2] J. R. Schrieffer, *Theory of Superconductivity* (Benjamin, New York, 1964).
- [3] E. W. Carlson, *et al.*, *Phys. Rev. Lett.* **83**, 612 (1999).
- [4] A. Mihlin and A. Auerbach, *Phys. Rev. B* **80**, 134521 (2009).
- [5] Samuele Sanna *et al.*, *Phys. Rev. B* **77**, 224511 (2008).
- [6] D. M. Broun, *et al.*, *Phys. Rev. Lett.* **99**, 237003 (2007).
- [7] W. N. Hardy, *et al.*, *Phys. Rev. Lett.* **70**, 3999 (1993).
- [8] Ch. Renner, *et al.*, *Phys. Rev. Lett.* **80**, 149 (1998).
- [9] J. Corson, *et al.*, *Nature* **398**, 221 (1999).
- [10] R. Timusk and B. Statt, *Rep. Prog. Phys.* **62**, 61 (1999).
- [11] A. Damascelli, Z. X. Shen and Z. Hussain, *Rev. Mod. Phys.* **75**, 473 (2003).
- [12] M. Le Tacon, *et al.*, *Nature* **2**, 537 (2006).
- [13] Subir Sachdev, *Science* **288**, 475 (2000).
- [14] Y. Wang, L. Li and N. P. Ong, *Phys. Rev. B* **73**, 024510 (2006).
- [15] J.M. Kosterlitz and D.J. Thouless, *J. Phys. C* **6** (1973) 1181; *J.M. Kosterlitz, J. Phys. C* **7** (1974) 1046.
- [16] P. W. Anderson, *Science* **316**, 1705 (2007).
- [17] G. Kotliar and A. E. Ruckenstein, *Phys. Rev. Lett.* **57**, 1362 (1986).
- [18] Miyake, K., Schmitt-Rink, S. Varma, C. M. *Phys. Rev. B* **34**, 6554 (1986). Moriya, T., Takahashi, Y. Ueda, K. *J. Phys. Soc. Jpn* **52**, 2905 (1990).
- [19] A. Alexandrov, *Theory of Superconductivity from Weak to Strong Coupling*, (Bristol&Philadelphia, 2003, 320 p).
- [20] Wei-Guo Yin, Chang-De Gong and P. W. Leung, *Phys. Rev. Lett.* **81**, 2534 (1998).
- [21] A. Ino, *et al.*, *Phys. Rev. B* **62**, 4137 (2000); *Phys. Rev. B* **65**, 094504 (2002).
- [22] T. Yoshida, *et al.*, *Phys. Rev. B* **74**, 224510 (2006); *Phys. Rev. Lett.* **103**, 037004 (2009).
- [23] W. J. Padilla, *et al.*, *Phys. Rev. B* **72**, 060511(R) (2005).
- [24] Yucel Yildirim and Wei Ku, *Phys. Rev. X* **1**, 011011 (2011).
- [25] Niedermayer, Ch. *et al.* *Phys. Rev. Lett.* **80**, 3843 (1998).
- [26] Elbio Dagotto, *et al.* *Phys. Rev. Lett.* **74**, 310 (1995).
- [27] P. W. Anderson, *Science* **235**, 1196 (1987).
- [28] H. A. Beth, *Z. Physik* **71**, 205 (1931).
- [29] T. Yoshida, *et al.*, *Phys. Rev. Lett.* **91**, 027001 (2003).
- [30] K. M. Shen, *et al.*, *Science* **307**, 901 (2005).
- [31] This is compatible to a previous study of the t' - J model. R. M. Fye, G. B. Martins and E. Dagotto, *Phys. Rev. B* **69**, 224507 (2004).
- [32] Gain in the effective kinetic energy of the pairs should lower the bare kinetic energy of the system as well. J.E. Hirsch, *Mod. Phys. Lett. B* **25**, 2219 (2011).
- [33] Kathleen M. Paget, *et al.*, *Phys. Rev. B* **59**, 641 (1999).
- [34] Yayu Wang, *et al.*, *Phys. Rev. Lett.* **95**, 247002 (2005).
- [35] J. E. Sonier, *et al.*, *Phys. Rev. B* **76**, 134518 (2007).
- [36] Yuri Zuev, Mun Seog Kim, and Thomas R. Lemberger, *Phys. Rev. Lett.* **95**, 137002 (2005).
- [37] Hai-Hu Wen, *et al.*, *Phys. Rev. B* **70**, 214505 (2004).
- [38] D. J. Pringle, G. V. M. Williams and J. L. Tallon, *Phys. Rev. B* **62**, 12527 (2000).